Membrane Cholesterol Modulates the Outward Facing Conformation of the Dopamine Transporter and Alters Cocaine Binding*[S]

Weimin C. Hong and Susan G. Amara[1]

From the Department of Neurobiology, University of Pittsburgh, Pittsburgh, Pennsylvania 15213

Clearance of synaptically released dopamine is regulated by the plasmalemmal dopamine transporter (DAT), an integral membrane protein that resides within a complex lipid milieu. Here we demonstrate that cholesterol, a major component of the lipid bilayer, can modulate the conformation of DAT and alter cocaine binding to DAT. In striatal synaptosomes and transfected cells, DAT was in cholesterol-rich membrane fractions after mild detergent extraction. After increasing the membrane cholesterol content by treatment of water-soluble cholesterol (cholesterol mixed with methyl-β-cyclodextrin), we observed an increase in DAT binding B_{max} values for cocaine analogs [^{3}H]WIN35428 and [^{125}I]RTI-55, but similar levels of DAT proteins on the cell surface were shown by surface biotinylation assays. Membrane cholesterol addition also markedly enhanced the accessibility of cysteine sulfhydryl moieties in DAT as probed by a membrane-impermeable maleimide-biotin conjugate. We identified cysteine 306, a juxtamembrane residue on transmembrane domain 6 (TM6) of DAT, as the intrinsic residue exhibiting enhanced reactivity. Similar effects on DAT cysteine accessibility and radioligand binding were observed with addition of zinc, a reagent known to promote the outward facing conformation of DAT. Using substituted cysteine mutants on various positions likely to be extracellular, we identified additional residues located on TM1, TM6, TM7, and TM12 of DAT that are sensitive to alterations in the membrane cholesterol content. Our findings in transfected cells and native tissues support the hypothesis that DAT adopts an outward facing conformation in a cholesterol-rich membrane environment, suggesting a novel modulatory role of the surrounding membrane lipid milieu on DAT function.

The dopamine transporter (DAT)[2] has a primary function to reaccumulate dopamine (DA) molecules into the presynaptic nerve terminal, thus limiting the extent and duration of DA signaling. Cocaine, a natural alkaloid from the leaves of the coca plant, is among the most widely abused drugs in modern society. Cocaine binds to DAT with high affinity and inhibits the transport of DA, resulting in prolonged DA neurotransmission in the brain. The enhanced DA signaling in the mesolimbic system is believed to be the main mechanism of action for cocaine addiction (1–3).

The DAT is a multispan integral membrane protein embedded in the plasmalemmal lipid bilayer, which comprises three main components: phospholipids, sphingolipids, and cholesterol. Cholesterol-rich domains within the membrane have been proposed to serve as a dynamic platform for membrane protein compartmentalization and organization (4, 5). Early reports have shown that the sodium-dependent uptake of γ-aminobutyric acid (GABA) by brain synaptosomes or reconstituted proteoliposomes requires membrane cholesterol (6, 7). Recent studies on the serotonin transporter, norepinephrine transporter, glycine transporter, and excitatory amino acid transporters (EAATs) have demonstrated that they can be associated with cholesterol-rich membrane domains in brain tissues or transfected cell lines (8–11). These reports have focused on the regulation of transporters under conditions in which membrane cholesterol is decreased by cholesterol-extracting agents such as methyl-β-cyclodextrin (MβCD). The substrate transport activity of these carriers is generally inhibited by cholesterol depletion. Association of DAT with cholesterol-rich membrane domains has been proposed to regulate the trafficking and lateral mobility of DAT in the membrane (12, 13).

Our laboratory has been interested in the modulation of neurotransmitter transporters by the surrounding lipid milieu and has shown previously that the electrophysiological properties of EAAT4 and DAT are modulated by arachidonate and polyunsaturated fatty acids (14, 15). In the current study, we examined whether altering the membrane cholesterol content can affect the function of DAT. We showed that moderate increases in the membrane cholesterol content in rat striatal synaptosomes and in cells transfected with DAT result in an increase in the number of binding sites for radiolabeled cocaine analogs and enhanced sulfhydryl accessibility of cysteine 306, a juxtamembrane residue on transmembrane domain 6 (TM6) of DAT. Using the substituted cysteine scanning method, we further demonstrated that the accessibility of cysteine residues introduced at multiple domains of DAT is influenced by changes in the membrane cholesterol content in a physiologically relevant range. Thus, we propose that in cholesterol-rich

[S] The on-line version of this article (available at http://www.jbc.org) contains supplemental Figs. 1 and 2.

[1] To whom correspondence should be addressed: Dept. of Neurobiology, University of Pittsburgh, 6068 BST3, 3501 Fifth Ave., Pittsburgh, PA 15213. Tel.: 412-383-8910; Fax: 412-383-5267; E-mail: amaras@pitt.edu.

[2] The abbreviations used are: DAT, dopamine transporter; DA, dopamine; wsChol, water-soluble cholesterol; MβCD, methyl-β-cyclodextrin; EAAT, excitatory amino acid transporter; TM, transmembrane domain; PEO$_2$, polyethylene oxide; WIN35428, (−)-2-β-carbomethoxy-3-β-(4-fluorophenyl)tropane; RTI-55, (−)-2β-carbomethoxy-3-β-(4-iodophenyl)tropane; NHS, N-hydroxysuccinimide.

membrane microdomains DAT adopts an outward facing conformation.

EXPERIMENTAL PROCEDURES

Chemicals, Radioligands, and Antibodies—Water-soluble cholesterol (wsChol), *i.e.* cholesterol mixed with MβCD (C4951, ~40–45 mg of cholesterol/g of MβCD), cholesterol-rich bovine serum (10–12 mg/ml cholesterol), and MβCD were from Sigma-Aldrich. Maleimide-PEO$_2$-biotin, sulfo-NHS-biotin, and NeutrAvidin-agarose beads were from Pierce. [^{3}H]DA (NET673, 16.9–30.6 Ci/mmol), [^{3}H]WIN35428 (NET1033, 85.9 Ci/mmol), and [^{125}I]RTI-55 (NEX272, 2200 Ci/mmol) were from Perkin-Elmer Life Sciences. All other chemicals were from Sigma-Aldrich or Fisher Scientific. The following antibodies were used in this study: anti-DAT (MAB369, Chemicon, Temecula, CA), anti-flotillin-1 (610820, BD Biosciences), anti-calnexin (sc-11397, Santa Cruz Biotechnology, Santa Cruz, CA), anti-β-actin (4967, Cell Signaling Technology, Beverly, MA), and anti-caveolin-1 (N-19, Santa Cruz Biotechnology). Rabbit antisera against DAT were generated using a GST fusion protein containing the DAT N-terminal sequence GVQLTSS-TLTNPRQSPVEAQDR (Covance, Denver, PA). The antisera specifically detected DAT immunoblot signals in rat striatal tissues without producing nonspecific signals in hippocampal or cortical tissues (16). Rabbit polyclonal antisera against EAAT3 were similarly generated using a GST fusion protein containing the intracellular C-terminal tail of human EAAT3. Horseradish peroxidase-conjugated secondary antibodies were from Jackson ImmunoResearch Laboratories (West Grove, PA) or Pierce.

Expression of DAT in Human Embryonic Kidney 293 (HEK293) and MN9D Cells—The coding sequence of human DAT cDNA was subcloned into pcDNA3.1(+) (Invitrogen) using KpnI and XbaI sites. Plasmid DNA was linearized with PvuI and transfected into HEK293 cells with FuGENE 6 reagent (Roche Applied Science). MN9D cells (immortalized mouse midbrain neurons expressing tyrosine hydroxylase, a generous gift from Drs. Heller and Won) were transfected with Lipofectamine 2000 (Invitrogen) and CombiMag (OZ Biosciences, Marseille, France). DAT-expressing clones were selected and maintained in DMEM (MediaTech, Manassas, VA) with 0.5 mg/ml G418, 10% fetal bovine serum (Hyclone, Logan, UT), and penicillin-streptomycin in humidified incubators with 5% CO$_2$ at 37 °C. DAT expression was verified by immunoblot and immunofluorescence staining with MAB369 antibodies.

Site-directed mutants of DAT were generated using the primer-based QuikChange method. Mutations were verified by standard DNA sequencing procedures. Mutant constructs were cloned into pcDNA3.1(+) and expressed in HEK293 cells by transient transfection or stable transfection when G418-resistant pools were selected.

Preparation of Rat Striatal Synaptosomes—Male Sprague-Dawley rats (200–250 g, Charles River) were euthanized, and striatal tissues were dissected. Tissues were rinsed in ice-cold HEPES-sucrose homogenization buffer (10 mM HEPES, pH 7.1, 0.32 M sucrose, 15 mM NaCl, 1× protease inhibitor mixture (Roche Applied Science)), resuspended in 20-fold (v/w) HEPES-sucrose homogenization buffer, and homogenized with a glass-

Teflon homogenizer at 5,000 rpm for 10–15 strokes. The homogenates were centrifuged at $1,000 \times g$ for 10 min at 4 °C. The supernatants were centrifuged at $30,000 \times g$ for 20 min at 4 °C. The resulting pellet (P2) was resuspended in 12-fold (v/w) HEPES-sucrose homogenization buffer, divided into aliquots, rapidly frozen in liquid N$_2$, and stored at −80 °C. All animal-related protocols were approved by the University of Pittsburgh Institutional Animal Use and Care Committee.

Methods for Altering Membrane Cholesterol Content—Freshly prepared MβCD or wsChol was dissolved in culture medium or appropriate buffer and added into 6-well or 96-well plates with confluent HEK-DAT or MN9D-DAT cells. The net weight of cholesterol in wsChol was calculated from the manufacturer's lot data. A solution of 50 μg/ml wsChol has an approximate concentration of 1 mM MβCD as carrier. After incubation at 37 °C, medium was aspirated, and cells were washed three times with cold PBSCM (PBS with 1 mM MgCl$_2$, 0.1 mM CaCl$_2$) before biotinylation or radioligand binding assays. Alternatively, cholesterol-rich bovine serum (10–12 mg/ml cholesterol) was added to wells in a 5 or 10% (v/v) ratio. Cholesterol contents in the lysates of cells and striatal synaptosomes were measured using the Amplex Red cholesterol assay kit (Invitrogen).

Striatal synaptosomes (~4.5 mg of protein/ml) were diluted 5-fold in appropriate buffer. Equal portions were incubated with vehicle, wsChol, or MβCD for 15 min at 37 °C. The synaptosomes were then spun down at $16,000 \times g$ for 10 min at 4 °C and resuspended in Tris-NaCl buffer (10 mM Tris-HCl, 150 mM NaCl, pH 7.5) for radioligand binding assays or in PBSCM for biotinylation assays.

Sucrose Gradient Flotation Centrifugation—Confluent HEK-DAT cells grown in 10-cm dishes were treated with MβCD or wsChol, washed with PBSCM, and solubilized with TNEB buffer (10 mM Tris, 150 mM NaCl, 1 mM EDTA, pH 7.5, 1% Brij-58) for 1 h at 4 °C. After a low speed spin of $1,000 \times g$ for 10 min, 0.3 ml of supernatants was mixed with 0.3 ml of TNEB containing 80% sucrose as the bottom fraction in 5-ml centrifuge tubes with 2.4 ml of 30% and 2 ml of 5% sucrose in TNEB buffer on top. The tubes were placed in an MLS-50 swing-bucket rotor and centrifuged at $160,000 \times g$ for 18 h at 4 °C in an Optima MAX ultracentrifuge (Beckman Coulter, Fullerton, CA). Twenty-four fractions (~200 μl/each) were collected from the bottom of the tube. Aliquots (15 μl) of each fraction were mixed with 4× SDS sample buffer, heated at 70 °C for 10 min, and loaded into 8–16% Tris-glycine-polyacrylamide gels (Invitrogen). Proteins were separated by electrophoresis, transferred to Immobilon-P PVDF membranes (Millipore, Billerica, MA), and probed with anti-DAT MAB369 (1:1,000 dilution) as primary antibody and HRP-conjugated goat anti-rat IgG as secondary antibody (1:2,000). The signals were visualized by Western Lightning chemiluminescence reagents (PerkinElmer Life Sciences) and digitized by a Chemi-DocIT imaging system (UVP, Upland, CA). The membranes were also probed with N-19 polyclonal antibodies (1:1,000) to detect caveolin-1.

Striatal synaptosomes (400 μl, ~4.5 mg of protein/ml) were mixed with 44 μl of 10% Brij-58 solution (Calbiochem) to achieve a final 1% concentration of Brij-58 and incubated for 1 h at 4 °C. After a low speed spin, 0.4 ml of supernatant was mixed

with 0.4 ml of TNEB buffer with 80% sucrose and loaded into a 5-ml tube with 2.2 ml of 30% and 2.0 ml of 5% sucrose in TNEB buffer on top. After centrifugation at $160,000 \times g$ for 18 h at 4 °C, 12 400-μl fractions were collected. Aliquots (20 μl) were subjected to SDS-PAGE, blotting, and probed with rabbit antisera against DAT (1:1,000 dilution), EAAT3 (1:1,000), and monoclonal antibody against flotillin-1 (1:1,000).

Surface Biotinylation—HEK-DAT or MN9D-DAT cells were seeded into 6-well plates and cultured to confluence. To improve cell attachment, plates were coated overnight with 0.05% polyethylenimine in borax-borate buffer, washed three times with deionized H$_2$O, and UV sterilized before seeding. Cells were treated with freshly prepared wsChol or MβCD, washed three times with cold PBS, and incubated with sulfo-NHS-biotin (1 mg/ml) in PBSCM (pH 8.0) or with maleimide-PEO$_2$-biotin (1 mg/ml) in PBSCM (pH 7.1) for 30–45 min at 4 °C. Zinc, cocaine, and other DAT inhibitors were included in the biotinylation buffer as indicated. The remaining sulfo-NHS-biotin or maleimide-PEO$_2$-biotin was quenched twice with PBSCM containing 100 mM glycine or 1 mM DTT for 15 min at 4 °C, respectively. After a final wash with PBS, cells were harvested and lysed in 330 μl of TNE lysis buffer (10 mM Tris, 150 mM NaCl, 1 mM EDTA, pH 7.5) with 1% Triton X-100 and protease inhibitors (Roche Applied Science) for 2 h at 4 °C followed by a 10-min centrifugation of $12,000 \times g$. The supernatants were divided into two portions: a 30-μl aliquot was saved as lysate input; the remaining 300 μl was incubated with 80 μl of a 50% slurry of NeutrAvidin-agarose beads (Pierce) overnight at 4 °C. The beads were washed one time with 400 μl of TNE lysis buffer and twice with 600 μl of PBS. The biotinylated proteins were eluted with 45 μl of SDS sample buffer at 70 °C for 10 min, separated by SDS-PAGE, transferred to PVDF membranes, and probed with MAB369 antibodies. Chemiluminescent images were analyzed with NIH ImageJ software to measure integrated density values of DAT bands. After subtracting the blank, the values were normalized to percentage of vehicle. Protein concentrations of lysates were routinely measured with a BCA kit (Pierce) for loading adjustment. Signals for calnexin, an endoplasmic reticulum-resident protein, or actin were also probed to verify membrane integrity during biotinylation.

Following cholesterol manipulation, striatal synaptosomes (~500 μg of total protein) were centrifuged and resuspended in 400 μl of PBSCM (pH 7.1) containing 5 mg/ml maleimide-PEO$_2$-biotin and incubated at 4 °C for 30 min. Cocaine was included during biotinylation as indicated. The remaining maleimide-PEO$_2$-biotin was quenched by adding 100 μl of PBSCM containing 500 mM cysteine and incubating for 15 min at 4 °C. After a 10-min centrifugation at $16,000 \times g$, the synaptosomes were resuspended in 330 μl of TNE lysis buffer. As noted above, biotinylated proteins were similarly affinity-purified and probed with rabbit polyclonal antisera for DAT and antibodies for actin.

[³H]WIN35428 Binding—HEK-DAT cells were seeded into polyethylenimine-coated 96-well plates and cultured to confluence. Cells were incubated with vehicle, freshly prepared wsChol at 50 μg/ml for 15 min, or cholesterol-rich bovine lipids (5%, v/v) for 1 h at 37 °C. After aspirating the medium, cells were washed with cold PBSCM using a plate washer (BioTek,

Winooski, VT) and incubated with PBSCM containing 7.5 nM [³H]WIN35428 and various concentrations of cocaine, unlabeled WIN35428, or other DAT inhibitors at 4 °C for 1.5 h. Cells were then washed once with cold PBSCM and lysed with 0.2 ml of scintillation mixture overnight. Bound radioactivity was determined by liquid scintillation spectrometry using a Wallac MicroBeta counter (PerkinElmer Life Sciences). Data were analyzed with GraphPad Prism 4.0 software (La Jolla, CA) for non-linear curve fitting.

[³H]DA Uptake—Following drug incubation or cholesterol treatment, confluent HEK-DAT or MN9D-DAT cells in 96-well plates were washed once with PBSCM. Uptake was initiated by adding 40 μl of PBSCM containing 50 nM [³H]DA, various concentrations of unlabeled DA, and 5 μM catechol-*O*-methyl transferase inhibitor Ro 41-0960. After incubation at room temperature for the indicated duration, the buffer was aspirated, and cells were washed once with 300 μl of PBSCM. Retained radioactivity was determined by liquid scintillation spectrometry. Data were analyzed using the Michaelis-Menten kinetic equation with GraphPad Prism 4.0.

[¹²⁵I]RTI-55 Binding—Following cholesterol manipulation, striatal synaptosomes were resuspended in Tris-NaCl buffer and aliquoted to a deep well microplate containing 0.1 nM [¹²⁵I]RTI-55, various concentrations of DAT inhibitors, and 0.5 μM fluoxetine in a total volume of 150 μl. After 3–4 h of incubation on ice, samples were applied to a 96-well harvester (Brandel, Gaithersburg, MD), rapidly filtrated onto 96-well GF/B UniFilter plates (Whatman) presoaked with 0.1% polyethylenimine, and washed four times with 1 ml of cold buffer (10 mM Tris-HCl, pH 7.5). Radioactivity retained on the filter was extracted overnight with 0.2 ml of scintillation mixture and determined with a Wallac MicroBeta counter.

RESULTS

DAT Exists in Cholesterol-rich Domains of Cell Membrane—A hallmark of membrane proteins associated with cholesterol-rich microdomains is that they are resistant to non-ionic detergent extraction at low temperature. We first tested the solubility of endogenously expressed DAT in striatal synaptosomes in the non-ionic detergent Brij-58. Rat striatal synaptosomes were treated with 1% Brij-58 at 4 °C for 1 h followed by sucrose gradient flotation centrifugation and fractionation. Detergent-solubilized DAT proteins were distributed in heavier sucrose fractions (from fractions 2 to 8), which contained most proteins including EAAT3, a glutamate transporter shown previously to be mostly solubilized by cold detergent extraction (10). However, the DAT was also present in fractions (from fractions 10 to 16) with high cholesterol concentrations and enriched in flotillin-1, a marker known to exist in cholesterol-rich membrane domains (Fig. 1*A*). Approximately 48% of total DAT was associated with detergent-resistant fractions (fractions 10–16) ($n = 2$). These data demonstrated that a substantial portion of DAT in native tissues resides in cholesterol-rich membrane domains.

Similar assays using stably transfected HEK293 cells expressing human DAT (HEK-DAT) also identified two pools of DAT (Fig. 1*B*). A major portion of glycosylated DAT (~85 kDa) resides in the more buoyant fractions (fractions 13–17) rich in cholesterol. The remaining DAT was solubilized by Brij-58 and
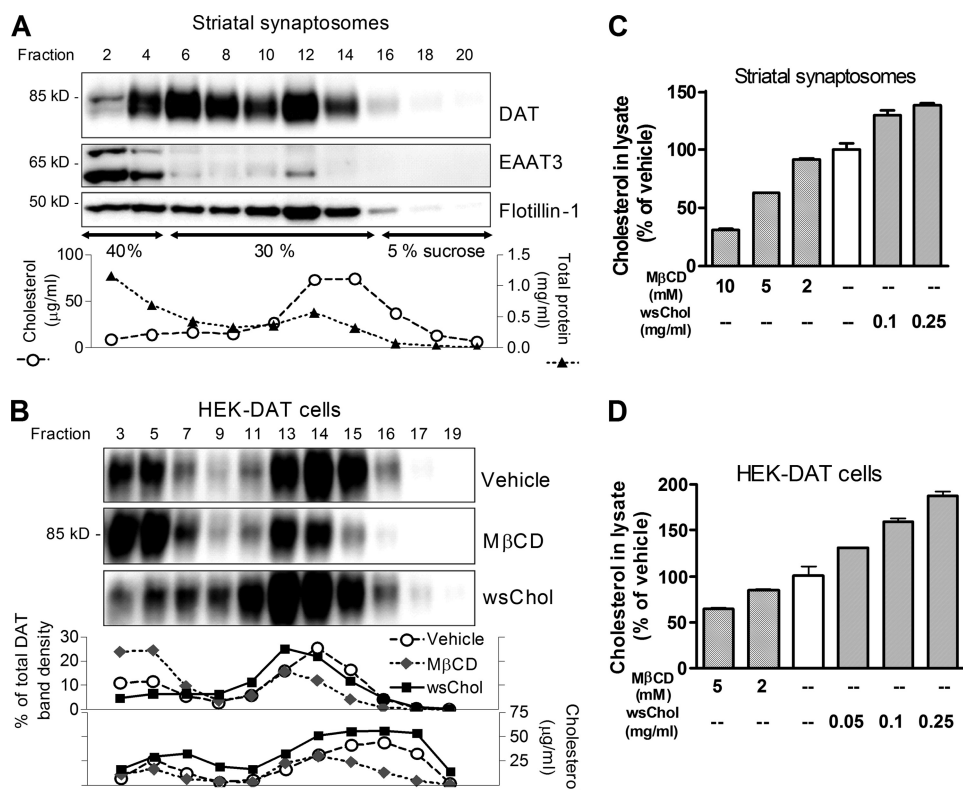
FIGURE 1. **DAT is associated with cholesterol-rich membrane domains.** *A*, rat striatal synaptosomes (1.8 mg of total protein) were treated with 1% Brij-58 at 4 °C for 1 h and subjected to discontinuous sucrose gradient flotation centrifugation. Twenty-four fractions were collected. Every other fraction was analyzed for protein (▲) and cholesterol (○) concentrations and immunoblotted for DAT, flotillin-1, and EAAT3. *B*, manipulation of the membrane cholesterol content in HEK-DAT cells shifts the distribution of DAT between detergent-solubilized and detergent-resistant cholesterol-rich fractions. Confluent cells in 10-cm dishes were treated with 5 mM MβCD or 0.25 mg/ml wsChol in culturing medium at 37 °C for 0.5 h and solubilized with 1% Brij-58 at 4 °C for 1 h. Band densities of DAT were quantified and converted to percentage of total signals within each treatment. *C* and *D*, measurement of cholesterol concentrations in HEK-DAT cell and striatal synaptosomes after a brief incubation with MβCD or wsChol. A dose of 0.1 mg/ml wsChol contains ~2 mM MβCD carrier. Cholesterol concentrations in lysates were normalized to percentage of vehicle control. Shown are averages ± S.D. (*error bars*) of triplicate samples from a representative assay.

distributed in heavier sucrose fractions (fractions 3–9). Extracting membrane cholesterol using MβCD altered the relative ratio of these two pools of DAT, whereas increasing the membrane cholesterol content using wsChol induced an opposite effect, shifting the distribution of DAT toward cholesterol-rich membrane fractions (Fig. 1*B*).

MβCD or wsChol treatment effectively altered the cholesterol content in HEK-DAT cells and striatal synaptosomes. After a brief incubation (15–30 min), the cholesterol concentrations in cell or synaptosomal lysates were decreased by MβCD or increased by wsChol in a dose-dependent manner (Fig. 1, *C* and *D*). Compared with HEK-DAT cells, synaptosomes require higher doses of MβCD or wsChol to change the cholesterol content. Although this assay measures the total cholesterol concentration in the lysates of cells or synaptosomes, it has been shown to provide a reasonable estimation of the cholesterol content in the plasma membrane, which represents the predominant pool of cholesterol in mammalian cells. In subsequent studies, we focused on the effects induced by a moderate increase (30–50% above control) in the cholesterol concentration at a dose of 0.05–0.1 mg/ml wsChol in HEK-DAT cells and 0.1 mg/ml wsChol in striatal synaptosomes.

Membrane Cholesterol Content Significantly Alters Cocaine Binding to DAT—We next examined whether the membrane cholesterol content could affect the binding of transport inhibitors such as cocaine to DAT. Whole-cell radioligand binding assays were performed using [3H]WIN35428, a cocaine analog, to measure specific binding of DAT in HEK-DAT cells. Non-linear regression (GraphPad Prism 4.0) of binding data revealed that the cocaine competition curve in vehicle preferred a two-site over a one-site binding model ($p < 0.01$). IC_{50} values of cocaine for the high affinity and low affinity [3H]WIN35428 binding sites were 4.9 nM and 1.1 μM, respectively, with the high affinity site accounting for 17 ± 5% of total binding. Following membrane cholesterol loading, the binding curves were statistically better fitted with a one-site model with an IC_{50} of 0.5 μM for cocaine in cells pretreated with 0.05 mg/ml wsChol or 1.1 μM in those preincubated with 5% (v/v) cholesterol-rich bovine lipids. In addition, total binding of [3H]WIN35428 was significantly increased to 117 ± 4 and 127 ± 6% of control, respectively (Fig. 2*A*). The cholesterol-induced increase in binding was observed using different concentrations of [3H]WIN35428 (ranging from 2.5 to 10 nM) or different NaCl concentrations (from 10 to 150 mM with choline chloride replacing NaCl) with higher doses of wsChol (0.1 mg/ml) or cholesterol-rich lipids (10%, v/v) producing a larger effect (data not shown). These data indicated that membrane cholesterol loading in HEK-DAT cells altered the binding profile of [3H]WIN35428 to DAT. A similar potentiating effect of wsChol on [3H]WIN35428 binding in rat striatal synaptosomes was also observed (data not shown).

[125I]RTI-55, another cocaine analog-based radioligand, produced a more robust signal and less nonspecific binding than [3H]WIN35428 in striatal synaptosomes, and generated cocaine competition curves better fitted to a single site. Treatment with wsChol did not alter the IC_{50} value of cocaine to compete for RTI-55 but significantly increased the total binding of [125I]RTI-55 by ~25% above vehicle ($n = 4$) (Fig. 2*B*). In homologous competition assays, the B_{max} of [125I]RTI-55 binding was increased by 20% in wsChol-treated samples compared with vehicle (Fig. 2*C*), whereas the K_d values were similar. This effect was specifically attributed to cholesterol, but not to the carrier molecule MβCD present in wsChol, because an equivalent dose of MβCD did not substantially change the B_{max} value.
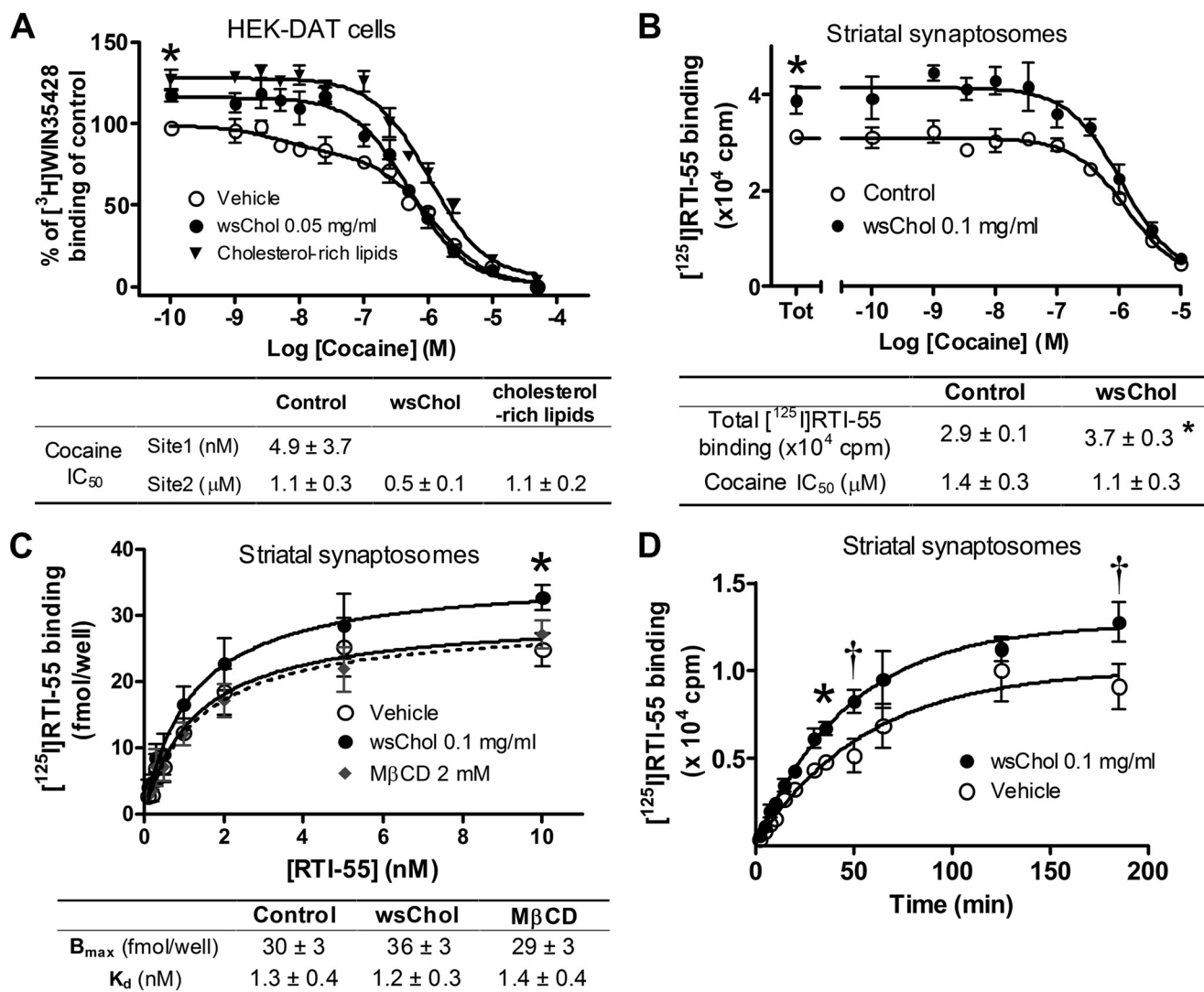
A HEK-DAT cells

		Control	wsChol	cholesterol-rich lipids
Cocaine IC$_{50}$	Site1 (nM)	4.9 ± 3.7		
	Site2 (μM)	1.1 ± 0.3	0.5 ± 0.1	1.1 ± 0.2

B Striatal synaptosomes

	Control	wsChol
Total [^{125}I]RTI-55 binding (x10^4 cpm)	2.9 ± 0.1	3.7 ± 0.3 *
Cocaine IC$_{50}$ (μM)	1.4 ± 0.3	1.1 ± 0.3

C Striatal synaptosomes

	Control	wsChol	MβCD
B$_{max}$ (fmol/well)	30 ± 3	36 ± 3	29 ± 3
K$_d$ (nM)	1.3 ± 0.4	1.2 ± 0.3	1.4 ± 0.4

D Striatal synaptosomes

FIGURE 2. **Membrane cholesterol content alters radioligand binding to DAT.** *A*, cocaine competition curves of [^{3}H]WIN35428 binding in HEK-DAT cells. Confluent cells were preincubated with wsChol (0.05 mg/ml; 15 min) or cholesterol-rich bovine lipids (5%, v/v; 1 h) at 37 °C and incubated with 7.5 nM [^{3}H]WIN35428 as described under "Experimental Procedures." The control curve was best fitted by a two-site competition *versus* a one-site model ($p < 0.01$), whereas the other two curves were best fitted to a one-site model with total binding significantly higher than control (*, $p < 0.05$; paired two-sided *t* test). [^{3}H]WIN35428 binding (cpm) was normalized to the total binding in control. Shown are the average ± S.E. values (*error bars*) from four independent experiments, each with triplicate or quadruplicate samples. Radioactivity bound to cells was less than 10% of total [^{3}H]WIN35428 added. Nonspecific binding measured in the presence of 10 μM mazindol was typically less than 20% of total binding. Non-linear curve fitting was done using GraphPad Prism 4.0. *B*, membrane cholesterol loading increases the number of [^{125}I]RTI-55 binding sites in rat striatal synaptosomes. Striatal synaptosomes were treated with vehicle or 0.1 mg/ml wsChol for 15 min at 37 °C and resuspended in Tris-NaCl buffer containing 0.1 nM [^{125}I]RTI-55 and various concentrations of cocaine for 3–4 h on ice. Competition curves from a representative experiment with triplicate samples are shown (average ± S.D.) with the summarized results (average ± S.E. (*error bars*)) from four experiments presented in the table *below*. Both curves favor a one-site fit when analyzed by non-linear regression. Bound radioactivity was less than 10% of total [^{125}I]RTI-55 added. Nonspecific binding measured in the presence of 10 μM mazindol was less than 10% of total binding. *, $p < 0.05$; two-sided *t* test. *C*, competition curves for [^{125}I]RTI-55 binding in rat striatal synaptosomes. Assays were similarly done to those in *B* except that unlabeled RTI-55 was used as a competition ligand. Effects of wsChol were not due to the cholesterol carrier MβCD because equivalent amounts of MβCD did not change [^{125}I]RTI-55 binding. *, $p < 0.05$; paired two-sided *t* test, wsChol *versus* vehicle. Shown are averages ± S.E. (*error bars*) from three to five experiments with quadruplicate samples. Nonspecific binding measured in the presence of 1 μM unlabeled RTI-55 was subtracted. *D*, time course of [^{125}I]RTI-55 binding in vehicle- or wsChol-treated striatal synaptosomes containing equal amounts of protein. The effect of wsChol was seen throughout the assay duration with steady state likely reached in 3 h. Shown are representative curves (average ± S.D. (*error bars*)) from two experiments, each with triplicate samples. †, $p < 0.01$; *, $p < 0.05$; two-way analysis of variance with post hoc Bonferroni test.

The association rates of RTI-55 in vehicle- or wsChol-treated synaptosomes were similar with wsChol-treated samples displaying an increase in [^{125}I]RTI-55 binding throughout the incubation from 5 min to 3 h when steady state was reached (Fig. 2*D*). The wsChol-induced increase in [^{125}I]RTI-55 B_{max} was reproducible when DAT-specific drugs such as WIN35428, bupropion, benztropine, dopamine, and amphetamine were used as competing ligands on ice or at room temperature (RT)

(supplemental Fig. 2). However, compared with cold incubation, reduced binding activities were seen following RT incubation in both vehicle and wsChol samples.

Accessibility of Sulfhydryl Side Chains of DAT Is Modulated by Membrane Cholesterol Content—The intriguing effects of membrane cholesterol on cocaine binding prompted us to investigate whether cholesterol might alter the conformation of DAT. We used maleimide-PEO$_2$-biotin, a membrane-imper-

meable surface biotin conjugate that selectively reacts with sulf-hydryl (−SH) moieties, to examine the accessibility of cysteine side chains in DAT from the extracellular aqueous environment. In parallel experiments, surface DAT was assessed using sulfo-NHS-biotin, a membrane-impermeable reagent that selectively labels multiple lysine side chains (primary amine, -NH$_2$) and is used to measure total DAT expression on the cell surface. Biotinylated proteins were affinity-purified, separated by SDS-PAGE, and probed with specific antibodies to examine the labeling of DAT via its -NH$_2$ or −SH side chains.

With moderate to low doses of wsChol treatment in HEK-DAT cells, comparable amounts of DAT were labeled by sulfo-NHS-biotin, indicating that there was no substantial change of the amount of DAT on the cell surface. However, an increase in DAT labeling by maleimide-PEO$_2$-biotin was observed in wsChol-treated samples (Fig. 3A), suggesting that −SH groups of certain cysteine residues in DAT become more accessible after membrane cholesterol loading. The rapid change of −SH accessibility was dependent on the dose of wsChol and the incubation duration (2.1- and 2.6-fold above vehicle for 3- and 10-min incubation with 50 μg/ml wsChol). Moreover, there was no evidence of compromised membrane permeability during the labeling because calnexin, an endoplasmic reticulum-resident protein, was not detected in biotinylated samples. This effect of wsChol was not due to the carrier MβCD because no significant change of cysteine reactivity was seen when cells were incubated with 2.5 mm MβCD for 0.5 h (data not shown).

We also used MN9D-DAT cells, which are derived from tyrosine hydroxylase-positive mouse midbrain neurons and stably transfected with human DAT. Following wsChol treatment, labeling of DAT by maleimide-PEO$_2$-biotin was enhanced to 3.7-fold above vehicle (Fig. 3B). Interestingly, the accessibility of intrinsic cysteine residues in DAT was also increased when the DAT inhibitor cocaine was present in the biotinylation buffer (4.8-fold above vehicle), and this effect was apparently additive with that of wsChol pretreatment (6.9-fold above vehicle). No change in reactivity was seen with benztropine, another DAT inhibitor with a different chemical structure.

Natively expressed DAT in rat striatal synaptosomes also exhibited increased sulfhydryl accessibility after the membrane cholesterol content was raised. Following wsChol treatment, synaptosomes were washed and incubated with maleimide-PEO$_2$-biotin. In comparison with vehicle control, enhanced DAT labeling (1.3 ± 0.1-fold of vehicle, $n = 2$) was seen in samples treated with wsChol (Fig. 3C).

Sulfhydryl Side Chain of Cysteine 306 in DAT Is Conformationally Sensitive to Membrane Cholesterol Content—We next sought to determine the specific cysteine residues on DAT that exhibit conformational sensitivity to the membrane cholesterol content. The solved crystal structure of LeuT$_{Aa}$, a prokaryotic ortholog of the DAT, has provided important insights into the overall architecture and substrate translocation mechanisms of the neurotransmitter sodium symporter family (17). Based on the predicted 12-TM topology (18) and the sequence alignment with LeuT$_{Aa}$, four cysteine residues in DAT are likely accessible from the extracellular hydrophilic side. Cysteines 180 and 189 in extracellular loop 2 (EL2) are proposed to form a disulfide
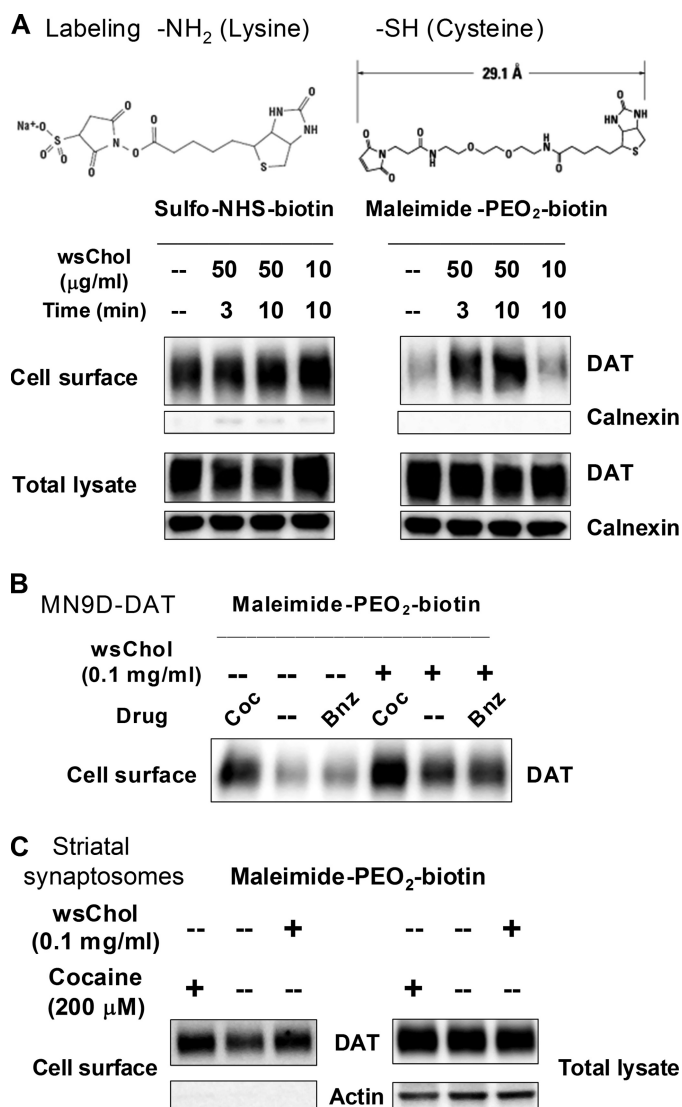

A Labeling -NH$_2$ (Lysine)   -SH (Cysteine)

FIGURE 3. **Membrane cholesterol content affects accessibility of cysteine sulfhydryl side chains of DAT.** *A*, wsChol treatment induces a rapid enhancement of −SH accessibility of DAT in HEK-DAT cells in a time- and dose-dependent manner. Following a brief incubation with wsChol, HEK-DAT cells were incubated with either 1 mg/ml sulfo-NHS-biotin or 1 mg/ml maleimide-PEO$_2$-biotin. Biotinylated proteins were affinity-purified, separated with SDS-PAGE, and immunoblotted using DAT- or calnexin-specific antibodies. Samples corresponding to $1/10$ of total cell lysates are also shown. *B*, wsChol treatment or cocaine binding enhances −SH accessibility of DAT in MN9D-DAT cells. Confluent MN9D-DAT cells were incubated with vehicle or 0.1 mg/ml wsChol in culture medium for 20 min at 37 °C, washed with cold PBSCM, and then biotinylated with 1 mg/ml maleimide-PEO$_2$-biotin. Cocaine (*Coc*; 100 μM) and benztropine (*Bnz*; 100 μM) were included during biotinylation. *C*, sulfhydryl accessibility of DAT in rat striatal synaptosomes is affected by the membrane cholesterol content. Striatal synaptosomes (0.5 mg of total protein) were incubated with vehicle or 0.1 mg/ml wsChol for 20 min at 37 °C, washed and resuspended in cold PBSCM, and then biotinylated with 5 mg/ml maleimide-PEO$_2$-biotin followed by lysis and affinity purification. Immunoblot signals in NeutrAvidin bead eluates and $1/8$ of total lysates were detected using rabbit antisera raised for DAT and actin. Chemiluminescent intensities of DAT bands were analyzed by ImageJ.

bond (19). We focused on Cys-90 and Cys-306 and generated their respective alanine mutants (C90A or C306A) using site-directed mutagenesis. When transiently transfected into HEK293 cells, wild-type (WT) or C90A DAT exhibited more labeling by maleimide-PEO$_2$-biotin following wsChol incubation. In contrast, the C306A mutant showed minimal

A

Maleimide-PEO$_2$-biotin
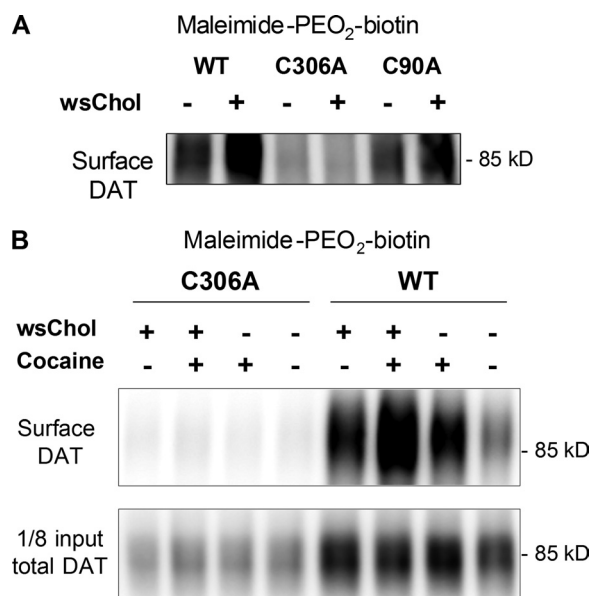

B

Maleimide-PEO$_2$-biotin

FIGURE 4. **Sulfhydryl side chain of Cys-306 in DAT exhibits conformational sensitivity to membrane cholesterol content.** *A*, representative blot (*n* = 3) from HEK293 cells transiently transfected with WT, C306A, and C90A DAT. Cells were treated with 0.1 mg/ml wsChol for 15 min at 37 °C and incubated with 1 mg/ml maleimide-PEO$_2$-biotin for 0.5 h at 4 °C. The enhanced biotinylation of sulfhydryl groups was not seen with the C306A mutant. *B*, HEK293 cells stably expressing wild-type and C306A DAT were probed with maleimide-PEO$_2$-biotin following wsChol treatment (0.05 mg/ml; 15 min at 37 °C). Where indicated, cocaine (1 mM) was included in the biotinylation buffer. Compared with the WT DAT, almost no biotinylated signals were detected with the C306A DAT. Despite its low expression level, C306A was expressed on the cell surface and exhibited functional substrate uptake and ligand binding (see Fig. 6*A*).

labeling under vehicle conditions, and no further changes were observed in wsChol-treated samples (Fig. 4*A*).

When stably transfected into HEK293 cells, C306A DAT was expressed at a lower level compared with WT DAT and displayed readily detectable [^{3}H]DA uptake (0.7 ± 0.1 pmol/well/min) and [^{3}H]WIN35428 binding (88 ± 6 fmol/well). In parallel biotinylation experiments, the WT DAT showed enhanced labeling after either wsChol incubation or cocaine incubation similar to the results with MN9D-DAT cells (Fig. 2*B*). The C306A DAT cells exhibited almost no labeling by maleimide-PEO$_2$-biotin (Fig. 4*B*). The absence of biotinylated signals demonstrated that Cys-306, a juxtamembrane residue just before TM6, is the main site for maleimide-PEO$_2$-biotin modification. Furthermore, its –SH side chain becomes more exposed to the extracellular aqueous environment following membrane cholesterol addition or cocaine binding. This is also consistent with previous observations that Cys-306 is accessible to methanethiosulfonate reagents applied from the extracellular side (20).

Both Zinc and wsChol Stabilize Outward Facing Conformation of DAT—Zinc has been reported to bind to an endogenous site in DAT and stabilize the outward facing conformation of DAT (21, 22). Micromolar concentrations of ZnCl$_2$ were shown to significantly increase [^{3}H]WIN35428 binding in transfected COS-7 cells with a maximal effect of ZnCl$_2$ observed at 10 μM (22). Because these effects were reminiscent of the results with wsChol in Fig. 2, we examined the possibility that wsChol and zinc might modulate the conformation of DAT in a similar way.

We compared the effects of wsChol and ZnCl$_2$ on radioligand binding in HEK-DAT cells. wsChol treatment before the binding assay increased the B_{max} value to 147 ± 26% of vehicle (*n* = 6). Inclusion of 10 μM ZnCl$_2$ in the binding buffer produced a dramatic increase in the B_{max} of [^{3}H]WIN35428 binding (215 ± 24% of vehicle, *n* = 6) without substantially changing the K_d (Fig. 5*A*).

Similar to early reports showing that zinc reduced uptake of [^{3}H]DA and [^{3}H]MPP$^+$ (1-methyl-4-phenylpyridinium) in cells transfected with DAT (22, 23), we also observed reduced [^{3}H]DA transport rates in HEK-DAT cells with uptake assays performed immediately following wsChol treatment. Compared with vehicle, preincubation with 0.1 mg/ml wsChol decreased the [^{3}H]DA uptake V_{max} value, whereas an equivalent dose of MβCD carrier had no significant effect (Fig. 5*B*).

We then performed surface biotinylation assays in HEK-DAT cells to examine the extracellular accessibility of DAT –SH moieties following application of wsChol or zinc. wsChol pretreatment significantly enhanced –SH reactivity in DAT (221 ± 12% of vehicle, *n* = 2). When 10 μM ZnCl$_2$ was included in the biotinylation buffer, increased labeling by maleimide-PEO$_2$-biotin (165 ± 11% of vehicle) was also observed (Fig. 5*C*). This effect was further potentiated when cells were pretreated with 0.05 mg/ml wsChol. Because parallel experiments using sulfo-NHS-biotin as a biotinylation agent showed comparable levels of DAT on the cell surface, these signals detected by maleimide-PEO$_2$-biotin reflected changes in cysteine accessibility in DAT. Similar to the results in Fig. 4*B*, cocaine also enhanced cysteine –SH reactivity (236 ± 39% of vehicle). These results from pharmacological and biochemical assays support the hypothesis that, like zinc, membrane cholesterol alters the conformation of DAT in a way that favors its outward facing orientation.

Membrane Cholesterol Has Global Influence on Conformation of Extracellular Domains of DAT—Our findings suggest that the conformation of DAT may be influenced by the surrounding lipid milieu, and we next sought to identify other DAT residues that display altered accessibility in cholesterol-rich membranes. Taking advantage of the observation that C306A DAT displayed almost no labeling by maleimide-PEO$_2$-biotin, we made a series of mutants containing single cysteine substitutions in different domains of DAT. Each of these mutants was generated within the background of C306A and contained an additional cysteine substitution in one of the several putative extracellular domains on DAT.

We constructed a structural model of human DAT based on its sequence homology with the prokaryotic ortholog LeuT$_{Aa}$ (17). The primary sequence of amino acid residues of human DAT (minus EL2) was threaded on the peptide backbone structure of LeuT$_{Aa}$ using the Swiss-PdbViewer program. When the DAT model was viewed from the extracellular side (Fig. 6*D*), we selected candidate residues for cysteine substitution whose side chains likely extend toward the aqueous environment and focused on TM6a and TM1b, which were proposed to gate the substrate permeation in LeuT$_{Aa}$. Several mutants (such as S309C/C306A, D313C/C306A, Y470C/C306A, and R85C/C306A) were found to be severely impaired in function. However, we identified four substituted cysteine mutants that
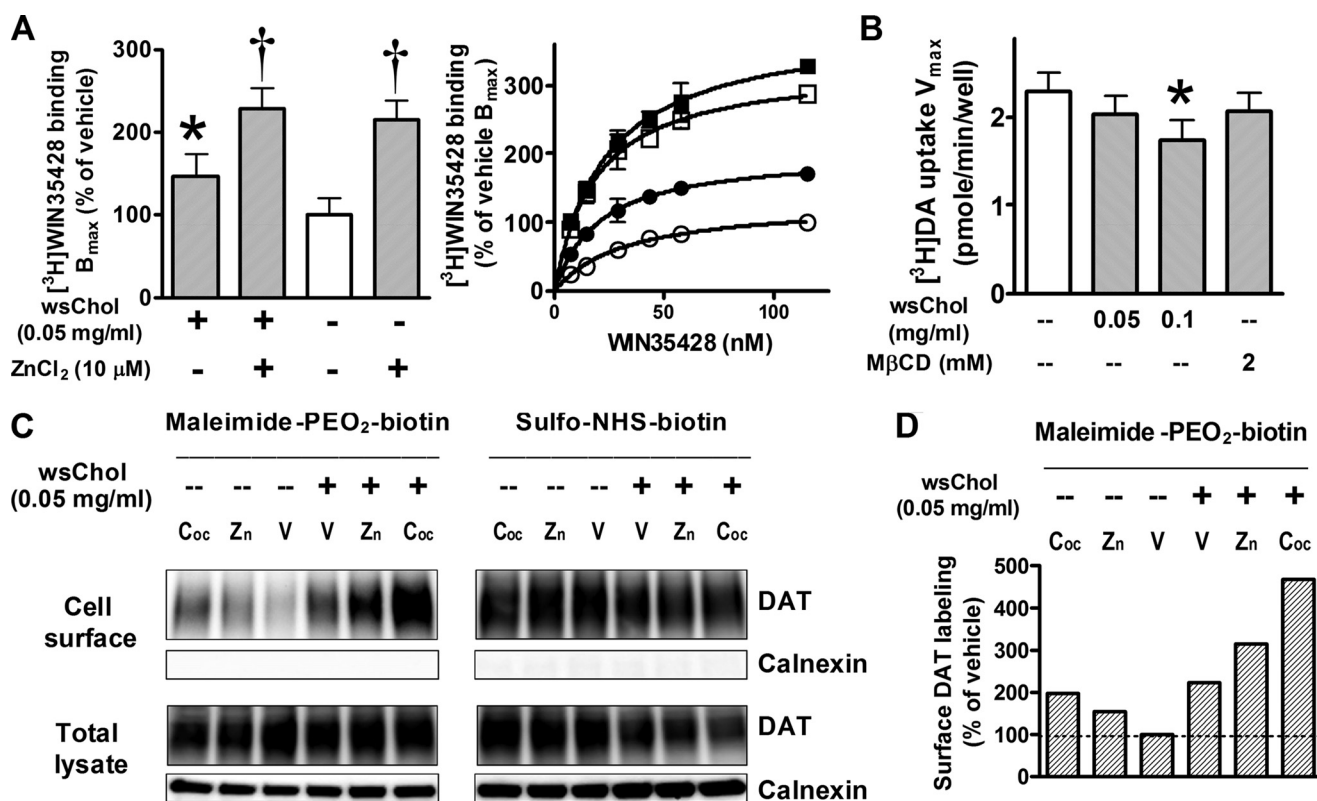
FIGURE 5. **Membrane cholesterol and zinc exert similar effects on cysteine accessibility and radioligand binding of DAT.** *A*, ZnCl$_2$ and wsChol treatment increases [^{3}H]WIN35428 binding B_{max} values in HEK-DAT cells. Following pretreatment with 0.05 mg/ml wsChol for 20 min, cells were incubated with binding buffer in the presence or absence of 10 μM ZnCl$_2$. *Left*, B_{max} values (average $\pm$ S.E.) normalized to percentage of vehicle. *, $p < 0.05$; †, $p < 0.01$; one-way analysis of variance and post hoc Dunnett's test; $n = 6$; each assay with triplicate samples. *Right*, representative binding curves (average $\pm$ S.D.) from an assay: ○, vehicle; ●, 0.05 mg/ml wsChol pretreatment; □, 10 μM ZnCl$_2$ included in binding buffer; ■, wsChol and ZnCl$_2$ combined. *B*, wsChol pretreatment (20 min) reduced [^{3}H]DA uptake V_{max} values in HEK-DAT cells. Shown are V_{max} values (average $\pm$ S.E. (*error bars*)) from six assays, each with triplicate samples. *, $p < 0.05$ compared with vehicle group; two-tailed *t* test. *C*, surface biotinylation results showed that zinc enhances DAT cysteine accessibility probed by maleimide-PEO$_2$-biotin, which was further enhanced by pretreatment with wsChol. Comparable surface DAT levels were detected by sulfo-NHS-biotin, a primary amine-selective biotinylation reagent. In contrast, sulfhydryl-selective maleimide-PEO$_2$-biotin revealed that inclusion of 1 mM cocaine (*Coc*) or 10 μM ZnCl$_2$ (*Zn*) increased cysteine side chain accessibility compared with vehicle (*V*), which was further potentiated when cells were pretreated with 0.05 mg/ml wsChol. Immunoblot signals in NeutrAvidin bead eluates and ^{1}/$_8$ of total lysates were detected using MAB369 for DAT and rabbit polyclonal antibody for calnexin. *D*, quantification of immunoblot signals of surface DAT labeling by maleimide-PEO$_2$-biotin shown in *C* (normalized to percentage of vehicle).

displayed robust [^{3}H]DA uptake and [^{3}H]WIN35428 binding (Fig. 6*A*). Interestingly, all four mutants exhibited differential cysteine sulfhydryl accessibility to membrane cholesterol and/or to cocaine incubation in biotinylation assays using maleimide-PEO$_2$-biotin.

When threonine 316 in the middle of TM6a was mutated to cysteine, the mutant T316A/C306A showed decreased labeling with maleimide-PEO$_2$-biotin after wsChol incubation but increased labeling in the presence of cocaine (Fig. 6*B*). The mutant K92C/C306A, in which cysteine replaced lysine 92 in the beginning of TM2, exhibited more labeling following either wsChol or cocaine treatment. The mutant A372C/C306A, containing a substituted cysteine at the end of TM7, showed significant enhancement of –SH accessibility to maleimide-PEO$_2$-biotin after incubation with wsChol but no change during cocaine incubation. When tryptophan 556 at the top of TM12 was mutated to cysteine, W556C/C306A exhibited decreased labeling after either wsChol or cocaine treatment. These results demonstrate that after membrane cholesterol loading some domains of DAT such as the end of TM7 and top of TM1b become more accessible from the extracellular side, whereas the middle section of

TM6a and top of TM12 become less accessible, suggesting that the conformational state when DAT resides in a cholesterol-rich membrane environment involves a more global change in the orientation of extracellularly facing residues (Fig. 6, *C* and *D*). In addition, because several residues (including Thr-316 and Ala-372) showed different patterns of labeling induced by wsChol treatment or by cocaine binding, these results also suggest that cholesterol and cocaine modulate DAT conformation in distinct ways.

DISCUSSION

Many integral membrane proteins and glycosylphosphatidyl-inositol-anchored proteins have been shown to be present in specialized membrane domains rich in cholesterol and sphingolipids. As a cell biological criterion, "lipid rafts" are resistant to extraction by non-ionic detergents such as Triton X-100 at a low temperature. However, the more general category of lipid microdomains defined as detergent-resistant membranes have been shown to exhibit heterogeneous sensitivities to different detergent extractions (24, 25). Our observations indicate that DAT is partially distributed within cholesterol-rich membrane domains resistant to extraction by a mild detergent, Brij-58.

A

	[³H]DA uptake		[³H]WIN35428 binding		
	V_{max} (pmol/min/well)	Log K_m (M)	B_{max} (fmol/well)	Log K_D (M)	V_{max} / B_{max} (molecule/sec)
Wild-type DAT	2.3 ± 0.2	-5.6 ± 0.1	333 ± 36	-7.2 ± 0.1	0.12 ± 0.01
C306A	0.7 ± 0.1	-5.9 ± 0.1	88 ± 6	-7.8 ± 0.1	0.14 ± 0.01
K92C / C306A	0.8 ± 0.1	-5.7 ± 0.1	36 ± 4	-8.9 ± 0.2	0.37 ± 0.05
T316C / C306A	2.0 ± 0.2	-5.8 ± 0.1	90 ± 4	-7.9 ± 0.1	0.37 ± 0.05
A372C / C306A	2.2 ± 0.2	-5.7 ± 0.1	157 ± 4	-7.9 ± 0.1	0.23 ± 0.02
W556C / C306A	1.1 ± 0.2	-6.1 ± 0.1	74 ± 6	-8.2 ± 0.1	0.26 ± 0.04

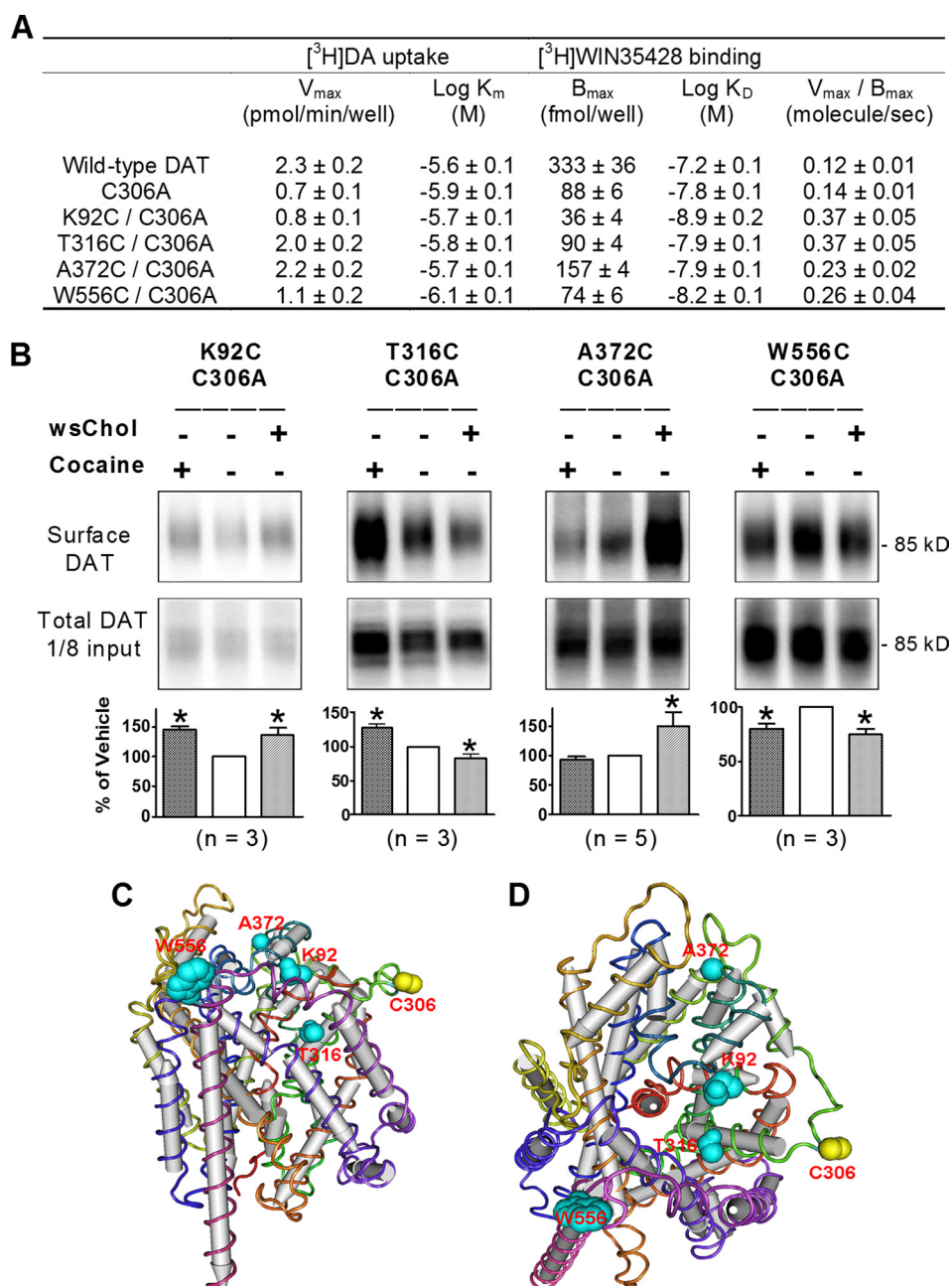FIGURE 6. **Membrane cholesterol addition or cocaine binding alters conformation of multiple DAT domains.** *A*, [³H]DA uptake activities and [³H]WIN35428 binding profiles of DAT wild type, C306A, and cysteine substitution mutants. Shown are means ± S.E. from three to eight experiments, each with triplicate samples. B) Four cysteine substitution mutations introduced into different domains of DAT exhibit distinct conformational sensitivities. Representative immunoblots of cell surface DAT probed by maleimide-PEO₂-biotin. Transfected HEK293 cells were pre-incubated with 0.1 mg/ml wsChol for 15 min at 37 °C, and biotinylated with maleimide-PEO₂-biotin at 4 °C for ~ 0.5 h. When indicated, cocaine (1 mM) was included in the biotinylation buffer. Biotinylated proteins were affinity-purified, separated by SDS-PAGE, and blotted with MAB369 for DAT. For each mutant, the integrated densities of DAT bands were quantified by ImageJ and normalized to those of vehicle treatment as 100%. Shown are averages ± S.E. from three to five experiments. *, $p < 0.05$ compared with vehicle; one-way analysis of variance and post hoc Dunnett's test. *C* and *D*, structural models of human DAT, based on the prokaryotic ortholog LeuT$_{Aa}$, observed from the membrane plane (*C*) or from the extracellular side (*D*). Based on sequence homology, the amino acid residues of human DAT (minus EL2) were threaded on the peptide backbone structure of LeuT$_{Aa}$ using the Swiss-PdbViewer program. The side chain of residues identified above are shown as space-filling models in *cyan* with cysteine 306 highlighted in *yellow*.

lower concentrations of Triton X-100 (0.1 or 0.5%) were used to show the association of DAT with detergent-resistant membranes (12, 13). We speculate that the association of DAT with cholesterol-rich membranes may be similar to that of SNARE proteins, which are known to be concentrated in cholesterol-dependent clusters in PC12 cells but are largely susceptible to cold Triton X-100 extraction (26).

In this study, we used moderate doses of wsChol, cholesterol-rich lipids, and MβCD, which increased or decreased the cholesterol content by up to 50% in cells and synaptosomes. Such changes in the cholesterol content potentially fall in the physiologically relevant range, considering the wide variations of plasma cholesterol levels detected among the human population (27). In cases where cholesterol homeostasis in the body is severely impaired such as familial hypercholesterolemia and Niemann-Pick diseases the patients' plasma cholesterol levels are severalfold higher than normal.

Using the substituted cysteine accessibility method and methanethiosulfonate reagents, it was previously demonstrated that Cys-90 and Cys-306 of DAT were accessible from the extracellular side and that cocaine binding affected the reactivity of Cys-90 (20). Others have shown that benztropine and cocaine differentially protected cysteine mutants from modification by methanethiosulfonate reagents, suggesting that the two drugs induce different conformational changes in the DAT (28). Here we used maleimide-PEO₂-biotin, which selectively and irreversibly reacts with sulfhydryl groups, and because its 29-Å spacer contains hydrophilic polyethylene oxide moieties, it is membrane-impermeant. Our results indicate that it specifically reacts with Cys-306, but not Cys-90, in human DAT. Although Cys-90

However, the association of DAT with detergent-resistant membranes does not appear to fulfill the strict criterion for lipid rafts. When treated with cold Triton X-100, DAT was almost completely solubilized (supplemental Fig. 1). In early reports, has been shown to react with smaller methanethiosulfonate reagents, the orientation of its thiol group in the DAT tertiary structure model (based on its prokaryotic ortholog LeuT$_{Aa}$) may be difficult for maleimide-PEO₂-biotin to access. In con-

trast, Cys-306 is located in a more open area near the extracellular side of TM6a with its sulfhydryl more exposed.

Because the C306A mutant of DAT does not react with externally applied maleimide-PEO$_2$-biotin, we engineered a series of substituted cysteine mutants within the C306A background. The sulfhydryl accessibility of these mutants suggests that in cholesterol-rich membranes the conformational rearrangements of DAT involve multiple domains. Specifically, it appears that the tilting of TM6a is influenced by membrane cholesterol because Cys-306 on the top of TM6a exhibited enhanced reactivity, whereas Thr-316 in the middle of TM6a showed reduced sulfhydryl reactivity. The mutant K92C, located at the extracellular end of TM1b, displayed increased sulfhydryl accessibility by either cholesterol loading or cocaine binding. Previous work on serotonin transporter and the GABA transporter probed the accessibility of substituted cysteine residues and suggested that TM1 and TM6 of SLC6 transporters may form part of the substrate permeation pathway (29–31). The altered accessibility of residues in TM6a and TM1b in our assays also hints that these domains could undergo structural rearrangements in response not only to inhibitor binding but also to surrounding lipid composition. Indeed, a recent study has resolved the structure of LeuT$_{Aa}$ with a bound competitive inhibitor and postulated a model in which TM1b, TM2a, and TM6a of the prokaryotic transporter undergo substantial conformational changes (32).

We explored the possibility that membrane cholesterol regulates the dynamic equilibrium between "outward facing" and "inward facing" conformations of DAT in the membrane using radioligand binding assays. Following membrane cholesterol loading at 37 °C, the binding assays were performed on ice to limit the conformational transitions of the DAT in cholesterol-rich membranes. Our results show that binding of cocaine analogs [^{125}I]RTI-55 and [^{3}H]WIN35428 in striatal synaptosomes and HEK-DAT cells is significantly increased when the membrane cholesterol content is augmented by treatment with wsChol or cholesterol-rich lipids. Competitive binding assays using DAT inhibitors and substrates indicated that the effect was specifically attributable to DAT, and it results from a change in B_{max}, not K_d, values for DAT radioligands. The increase in B_{max} by wsChol pretreatment was also observed when the binding assays was performed at RT. However, B_{max} values for either vehicle- or wsChol-treated samples were reduced to approximately half of those from assays done on ice, a condition at which protein degradation was minimized. As the recent LeuT$_{Aa}$ structure predicts that competitive inhibitors bind and trap the transporter in the "open-to-out" conformation (32), our results suggest that cholesterol-rich membranes provide an environment that favors an outward facing conformation of DAT, thus increasing the number of binding sites for radiolabeled inhibitors.

This hypothesis is further strengthened when we compared the effects of wsChol with zinc, which has been reported to stabilize an outward facing conformation of DAT (21, 22). There was a striking similarity between the effects of zinc and wsChol in our assays. First, both zinc and wsChol increased B_{max} values but did not change K_d values in radioligand binding assays done in HEK-DAT cells. Second, both treatments

enhanced the cysteine sulfhydryl reactivity of DAT when probed by maleimide-PEO$_2$-biotin.

We also observed a reduced [^{3}H]DA uptake rate in wsChol-treated HEK-DAT cells when the assay was done in 1.5-min duration at RT. It is plausible that following wsChol incubation the membrane microenvironment promotes the outward facing conformation of DAT and/or creates an energy barrier that limits the conversion of DAT to its inward facing conformation, resulting in an apparent decrease of substrate translocation rates. Surprisingly, no significant reduction of V_{max} values was seen when [^{3}H]DA uptake assays were done with longer durations such as 5 min at RT. It can be speculated that at RT the membrane dynamics of the cell may quickly alter the cholesterol-rich microenvironment surrounding DAT within minutes, thus diluting the initial effects imposed by wsChol. Such rapid effects exerted by membrane cholesterol may be better examined by electrophysiological methods or fluorescence measurements that can resolve events on faster time scales.

The readily reproducible two-site fit of [^{3}H]WIN35428 binding in HEK-DAT cells is somewhat intriguing. We observed IC$_{50}$ values of the competition of cocaine for [^{3}H]WIN35428 in a range similar to those in earlier reports showing that [^{3}H]WIN35428 exhibited high and low affinity sites in primate and rat caudate preparations (33, 34) and in COS cells transfected with rat DAT cDNA (35). Our binding data in striatal synaptosomes using [^{125}I]RTI-55, however, were better fitted by a one-site competition model regardless of cholesterol treatment. The discrepancy between DAT binding profiles of these two preparations could be attributed to the different membrane lipid environment between native neuronal tissues and transfected cells, which further strengthens the notion that membrane lipid milieu can modulate the conformational states of DAT and affect the binding affinities of DAT inhibitors such as cocaine.

Over the decades, many reports have suggested that cholesterol is important for the function of membrane proteins. The nicotinic acetylcholine receptor from *Torpedo* electric eels was extensively studied in liposome reconstitution experiments and exhibited a requirement of membrane cholesterol for ion flux (36, 37). Molecular dynamics simulation predicts that cholesterol molecules are embedded in multiple sites of acetylcholine receptor subunit assembly and are energetically favored to stabilize the native structure of acetylcholine receptor (38). In the recently solved structures of the β_2-adrenergic receptor, cholesterol molecules were present in the dimeric interface (39) or in a cleft formed by transmembrane helices and thought to stabilize the conformation of the protein (40). Stimulation of reconstituted GABA transport in liposomes by stoichiometric amounts of cholesterol suggested a structural requirement of GABA transporter for cholesterol (7). In this study, we demonstrate that membrane cholesterol modulates the protein conformation of DAT and significantly alters cocaine binding to DAT. Can cholesterol binding play a vital role in maintaining the native conformation of DAT? The possibility of such precise interactions between cholesterol and DAT eventually may be resolved in functional reconstitution assays and elucidated when the atomic structures of mammalian neurotransmitter transporters and their associated lipids become available.

REFERENCES

1. Ritz, M. C., Lamb, R. J., Goldberg, S. R., and Kuhar, M. J. (1987) *Science* **237,** 1219–1223
2. Torres, G. E., Gainetdinov, R. R., and Caron, M. G. (2003) *Nat. Rev. Neurosci.* **4,** 13–25
3. Mortensen, O. V., and Amara, S. G. (2003) *Eur. J. Pharmacol.* **479,** 159–170
4. Brown, D. A., and London, E. (1998) *Annu. Rev. Cell. Dev. Biol.* **14,** 111–136
5. Simons, K., and Ikonen, E. (1997) *Nature* **387,** 569–572
6. North, P., and Fleischer, S. (1983) *J. Biol. Chem.* **258,** 1242–1253
7. Shouffani, A., and Kanner, B. I. (1990) *J. Biol. Chem.* **265,** 6002–6008
8. Jayanthi, L. D., Samuvel, D. J., and Ramamoorthy, S. (2004) *J. Biol. Chem.* **279,** 19315–19326
9. Magnani, F., Tate, C. G., Wynne, S., Williams, C., and Haase, J. (2004) *J. Biol. Chem.* **279,** 38770–38778
10. Butchbach, M. E., Tian, G., Guo, H., and Lin, C. L. (2004) *J. Biol. Chem.* **279,** 34388–34396
11. Núñez, E., Alonso-Torres, P., Fornés, A., Aragón, C., and López-Corcuera, B. (2008) *J. Neurochem.* **105,** 2080–2090
12. Adkins, E. M., Samuvel, D. J., Fog, J. U., Eriksen, J., Jayanthi, L. D., Vaegter, C. B., Ramamoorthy, S., and Gether, U. (2007) *Biochemistry* **46,** 10484–10497
13. Foster, J. D., Adkins, S. D., Lever, J. R., and Vaughan, R. A. (2008) *J. Neurochem.* **105,** 1683–1699
14. Fairman, W. A., Sonders, M. S., Murdoch, G. H., and Amara, S. G. (1998) *Nat. Neurosci.* **1,** 105–113
15. Ingram, S. L., and Amara, S. G. (2000) *J. Neurosci.* **20,** 550–557
16. Padmanabhan, S., Lambert, N. A., and Prasad, B. M. (2008) *Eur. J. Neurosci.* **28,** 2017–2027
17. Yamashita, A., Singh, S. K., Kawate, T., Jin, Y., and Gouaux, E. (2005) *Nature* **437,** 215–223
18. Amara, S. G., and Kuhar, M. J. (1993) *Annu. Rev. Neurosci.* **16,** 73–93
19. Chen, R., Wei, H., Hill, E. R., Chen, L., Jiang, L., Han, D. D., and Gu, H. H. (2007) *Mol. Cell. Biochem.* **298,** 41–48
20. Ferrer, J. V., and Javitch, J. A. (1998) *Proc. Nat. Acad. Sci. U.S.A.* **95,** 9238–9243
21. Liang, Y. J., Zhen, J., Chen, N., and Reith, M. E. (2009) *J. Neurochem.* **109,** 981–994
22. Norregaard, L., Frederiksen, D., Nielsen, E. O., and Gether, U. (1998) *EMBO J.* **17,** 4266–4273
23. Scholze, P., Nørregaard, L., Singer, E. A., Freissmuth, M., Gether, U., and Sitte, H. H. (2002) *J. Biol. Chem.* **277,** 21505–21513
24. Pike, L. J. (2004) *Biochem. J.* **378,** 281–292
25. Schuck, S., Honsho, M., Ekroos, K., Shevchenko, A., and Simons, K. (2003) *Proc. Nat. Acad. Sci. U.S.A.* **100,** 5795–5800
26. Lang, T., Bruns, D., Wenzel, D., Riedel, D., Holroyd, P., Thiele, C., and Jahn, R. (2001) *EMBO J.* **20,** 2202–2213
27. Brown, M. S., Kovanen, P. T., and Goldstein, J. L. (1981) *Science* **212,** 628–635
28. Reith, M. E., Berfield, J. L., Wang, L. C., Ferrer, J. V., and Javitch, J. A. (2001) *J. Biol. Chem.* **276,** 29012–29018
29. Zhou, Y., Bennett, E. R., and Kanner, B. I. (2004) *J. Biol. Chem.* **279,** 13800–13808
30. Henry, L. K., Adkins, E. M., Han, Q., and Blakely, R. D. (2003) *J. Biol. Chem.* **278,** 37052–37063
31. Rosenberg, A., and Kanner, B. I. (2008) *J. Biol. Chem.* **283,** 14376–14383
32. Singh, S. K., Piscitelli, C. L., Yamashita, A., and Gouaux, E. (2008) *Science* **322,** 1655–1661
33. Madras, B. K., Spealman, R. D., Fahey, M. A., Neumeyer, J. L., Saha, J. K., and Milius, R. A. (1989) *Mol. Pharmacol.* **36,** 518–524
34. Gracz, L. M., and Madras, B. K. (1995) *J. Pharmacol. Exp. Ther.* **273,** 1224–1234
35. Boja, J. W., Markham, L., Patel, A., Uhl, G., and Kuhar, M. J. (1992) *Neuroreport* **3,** 247–248
36. Dalziel, A. W., Rollins, E. S., and McNamee, M. G. (1980) *FEBS Lett.* **122,** 193–196
37. Barrantes, F. J. (2007) *J. Neurochem.* **103,** Suppl. 1, 72–80
38. Brannigan, G., Hénin, J., Law, R., Eckenhoff, R., and Klein, M. L. (2008) *Proc. Nat. Acad. Sci. U.S.A.* **105,** 14418–14423
39. Cherezov, V., Rosenbaum, D. M., Hanson, M. A., Rasmussen, S. G., Thian, F. S., Kobilka, T. S., Choi, H. J., Kuhn, P., Weis, W. I., Kobilka, B. K., and Stevens, R. C. (2007) *Science* **318,** 1258–1265
40. Hanson, M. A., Cherezov, V., Griffith, M. T., Roth, C. B., Jaakola, V. P., Chien, E. Y., Velasquez, J., Kuhn, P., and Stevens, R. C. (2008) *Structure* **16,** 897–905